UDK 669.14:621.793/.795:532.6
Original scientific article/Izvirni znanstveni članek

ISSN 1580-2949
MTAEC9, 50(2)269(2016)

INVESTIGATION OF THE ADHESION AND WEAR PROPERTIES OF BORIDED AISI H10 STEEL

PREISKAVA ADHEZIJE IN OBRABNIH LASTNOSTI BORIRANEGA JEKLA AISI H10

Ibrahim Gunes, Melih Ozcatal

Afyon Kocatepe University, Faculty of Technology, Department of Metallurgical and Materials Engineering, 03200 Afyonkarahisar, Turkey
igunes@aku.edu.tr

Prejem rokopisa – received: 2015-02-02; sprejem za objavo – accepted for publication: 2015-03-11

doi:10.17222/mit.2015.032

In the present study the effect of the boriding process on the adhesion and wear properties of AISI H10 steel has been investigated. The boride layer was characterized by light microscopy, X-ray diffraction and the Vickers microhardness. The X-ray diffraction analyses of the boride layers on the surface of the steels revealed the existence of the compounds FeB, Fe_2B, CrB, Cr_2B and MoB. Depending on the chemical composition of the steel, the boride-layer thickness on the surface of the AISI H10 steel was found to be 63.72 µm. The hardness of the boride compounds formed on the surface of the steels ranged from 1648 to 1964 $HV_{0.05}$, whereas the Vickers hardness value of the untreated steel was 306 $HV_{0.05}$. The wear tests were carried out in a ball-on-disc arrangement under dry-friction conditions at room temperature with an applied load of 10 N and with a sliding speed of 0.3 m s^{-1} for a sliding distance of 1000 m. It was observed that the wear rate of the borided and non-borided AISI H10 steels ranged from 3.15 mm^3/N m to 62.84 mm^3/N m.

Keywords: AISI H10, boriding, microhardness, adhesion, wear rate

V predstavljeni študiji je bil preiskovan vpliv postopka boriranja na adhezijo in obrabne lastnosti jekla AISI H10. Borirana plast je bila karakterizirana s svetlobno mikroskopijo, z rentgensko difrakcijo in z merjenjem mikrotrdote po Vickersu. Analiza z rentgensko difrakcijo borirane plasti na površini jekel je odkrila prisotnost spojin: FeB, Fe_2B, CrB, Cr_2B in MoB. Odvisno od kemijske sestave jekla je bila debelina borirane plasti na površini jekla AISI H10 okrog 63,72 µm. Trdota borovih spojin, ki so nastale na površini jekel, je bila med 1648 $HV_{0,05}$ do 1964 $HV_{0,05}$, medtem ko je bila Vickers trdota neobdelanega jekla 306 $HV_{0,05}$. Izvršeni so bili preizkusi obrabe z napravo s kroglico na plošči pri pogojih suhega trenja pri sobni temperaturi z uporabljeno obremenitvijo 10 N, s hitrostjo drsenja 0,3 m/s pri dolžini drsenja 1000 m. Hitrost obrabe boriranega in neboriranega jekla AISI H10 je bila v območju od 3,15 mm^3/N m do 62,84 mm^3/N m.

Ključne besede: AISI H10, boriranje, mikrotrdota, adhezija, hitrost obrabe

1 INTRODUCTION

Boriding is a thermochemical treatment in which boron atoms diffuse through the surface of metallic substrates. As boron is an element of relatively small size it diffuses into a variety of metals, including ferrous, non-ferrous and some superalloys.[1–5] The boriding process provides a high surface hardness as well as good wear properties in terms of adhesion, abrasion, and surface fatigue. The boriding treatment is carried out by heating substrates in the temperature range 973 K –1323 K for a period of time ranging from 0.5 h to 12 h. The boron is supplied to the material surface by a solid, liquid, gaseous or plasma medium.[6–9]

The wear and friction behaviors of borided steels are broadly dependent on the following surface and boriding conditions: boriding time and temperature, chemical composition, mechanical properties, physical structure, lubricant, surface roughness, etc. As a result of these conditions, the life of machine components may be affected. The efficiency, durability and reliability are improved by reducing the friction and wear rate through certain materials, surface modifications and lubricants.[10,11]

Boriding is used in numerous applications in industries such as the manufacturing of machine parts for plastics and food processing, packaging and tooling, as well as pumps and hydraulic machine parts, crankshafts, rolls and heavy gears, motor and car construction. The wear behavior of borided steels has been evaluated by a number of investigators.[12–16] However, there is no information about the friction and wear behaviors of borided AISI H10 steel. The main objective of this study was to investigate the effect of the boriding process on the wear behavior of borided AISI H10 steel. The structural, Daimler-Benz adhesion and tribological properties were investigated using light microscopy, XRD, SEM, EDS, microhardness tests and a ball-on-disc tribotester.

2 EXPERIMENTAL PROCEDURES

2.1 Boriding and characterization

The AISI H10 steel contained *w* (C) = 0.32 %, *w* (Cr) = 3.15 %, *w* (Mo) = 2.90 %, *w* (V) = 0.65 % and *w* (Mn) = 0.40 %. The test specimens were cut into Ø 25 mm × 8 mm discs, ground to 1200 G and polished using a diamond solution. The boriding heat treatment was

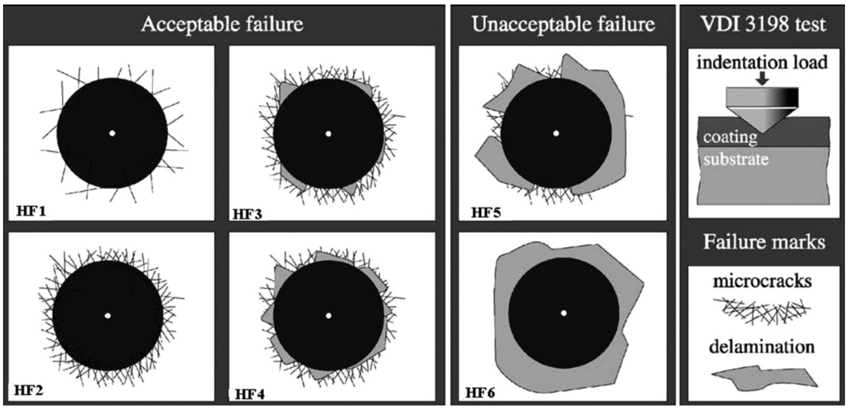

Figure 1: The principle of the VDI 3198 indentation test
Slika 1: Načelo VDI 3198 preizkusa vtiskovanja

carried out in a solid medium containing an Ekabor-II powder mixture placed in an electrical resistance furnace operated at temperatures of 1123 K and 1223 K for 2 h and 6 h under atmospheric pressure. The microstructures of polished and etched cross-sections of the specimens were observed under a Nikon MA100 light microscope. The presence of borides formed in the coating layer was confirmed by means of X-ray diffraction equipment (Shimadzu XRD 6000) using Cu–$K\alpha$ radiation. The hardness measurements of the boride layer on steel and an untreated steel substrate were made on the cross-sections using a Shimadzu HMV-2 Vickers indenter with a 50 g load.

The Daimler-Benz Rockwell-C adhesion test was used to assess the adhesion of the boride layers. This well-known Rockwell-C indentation test is prescribed by the VDI 3198 norm, as a destructive quality test for coated compounds.[17–20] The principle of this method is presented in the upper-right-hand part of **Figure 1**.[18] A load of 1471 N was applied to cause coating damage adjacent to the boundary of the indentation. Three indentations were conducted for each specimen and scanning electron microscopy was employed to evaluate the test.

2.2 Friction and wear

To perform the friction and wear of the borided samples a ball-on-disc test device was used. In the wear tests, WC-Co balls of 8 mm in diameter supplied by H. C. Starck Ceramics GmbH were used. Errors caused by the distortion of the surface were eliminated by using a separate abrasion element (WC-Co ball) for each test. The wear experiments were carried out in a ball-on-disc arrangement under dry-friction conditions at room temperature with an applied load of 10 N and with sliding speeds of 0.3 m s^{-1} for a sliding distance of 1000 m (track diameter 0.015 m). The wear tests were made with an 8-mm diameter WC–Co ball with a Young's modulus of 598 GPa. The maximum compressive contact pressure in the central point of the contact area was calculated from the Hertzian equation.[21] According to the Hertzian equation, the maximum contact pressures of 2824 MPa (for disc E_d = 325 GPa and ν_d = 0.26, for ball E_b = 598 GPa and ν_b = 0.22) were obtained at a normal load of 10 N. Before and after each wear test, each sample and abrasion element was cleaned with alcohol. After the test, the wear volumes of the samples were quantified by multiplying the cross-sectional areas of the wear by the width of the wear track obtained using a Taylor-Hobson Rugosimeter Surtronic 25 device. The wear rate was calculated with the following Equation (1):

$$W_k = \frac{Wv}{MS} \quad (\mathrm{mm^3/N\ m}) \tag{1}$$

where W_k is the wear rate, Wv is the worn volume, M is the applied load and S is the sliding distance. Friction coefficients depending on the sliding distance were obtained through a friction-coefficient program. The surface profiles of the wear tracks on the samples and the surface roughness were measured using a Taylor-Hobson Rugosimeter Surtronic 25. The worn surfaces were investigated using scanning electron microscopy

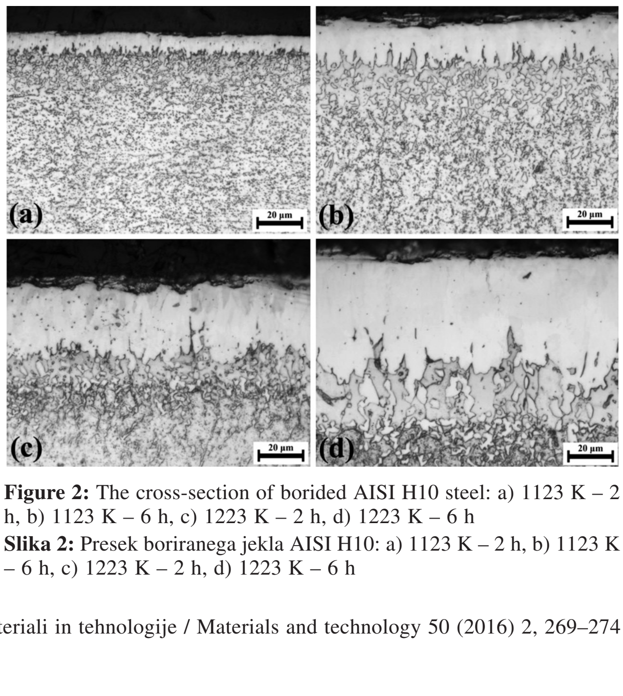

Figure 2: The cross-section of borided AISI H10 steel: a) 1123 K – 2 h, b) 1123 K – 6 h, c) 1223 K – 2 h, d) 1223 K – 6 h
Slika 2: Presek boriranega jekla AISI H10: a) 1123 K – 2 h, b) 1123 K – 6 h, c) 1223 K – 2 h, d) 1223 K – 6 h

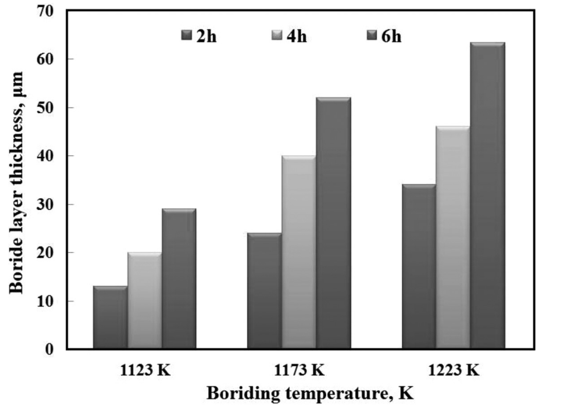

Figure 3: The thickness values of the boride layers with respect to boriding time and temperatures
Slika 3: Vrednosti debeline boriranih plasti glede na čas in temperaturo boriranja

(SEM), energy-dispersive X-ray spectroscopy (EDS) and a Nanovea ST-400 non-contact optical profiler.

3 RESULTS AND DISCUSSION

3.1 Characterization of the boride coatings

The cross-section light micrographs of the borided AISI H10 steel for temperatures of 1123 K and 1223 K for 2 h and 6 h are shown in **Figure 2**. As can be seen, the borides formed on the AISI H10 substrate have a saw-tooth morphology. It was found that the coating/matrix interface and the matrix could be easily distinguished and the boride layer had a columnar structure. Depending on the boriding time and temperature, the boride-layer thickness on the surface of the AISI H10 steel ranged from 12.86 μm and 63.72 μm (**Figure 3**).

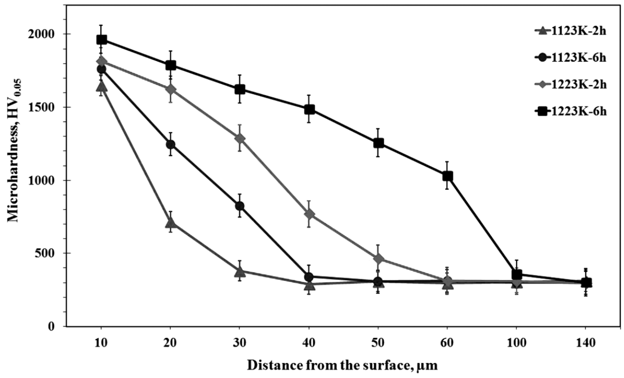

Figure 5: The variation of hardness depth in the borided AISI H10 steel
Slika 5: Spreminjanje trdote v globino pri boriranem jeklu AISI H10

Figure 4 shows the XRD pattern obtained from the surface of the borided AISI H10 steel at 1123 K and 1223 K for treatment times of 2 h and 6 h. The XRD patterns show that the boride layer consists of borides such as MB and M_2B (M=Metal; Fe, Cr). The XRD results showed that the boride layers formed on the H10 steel contained the FeB, Fe_2B, CrB, Cr_2B and MoB phases (**Figures 4a** and **4d**).

Microhardness measurements were carried out on cross-sections from the surface to the interior along a

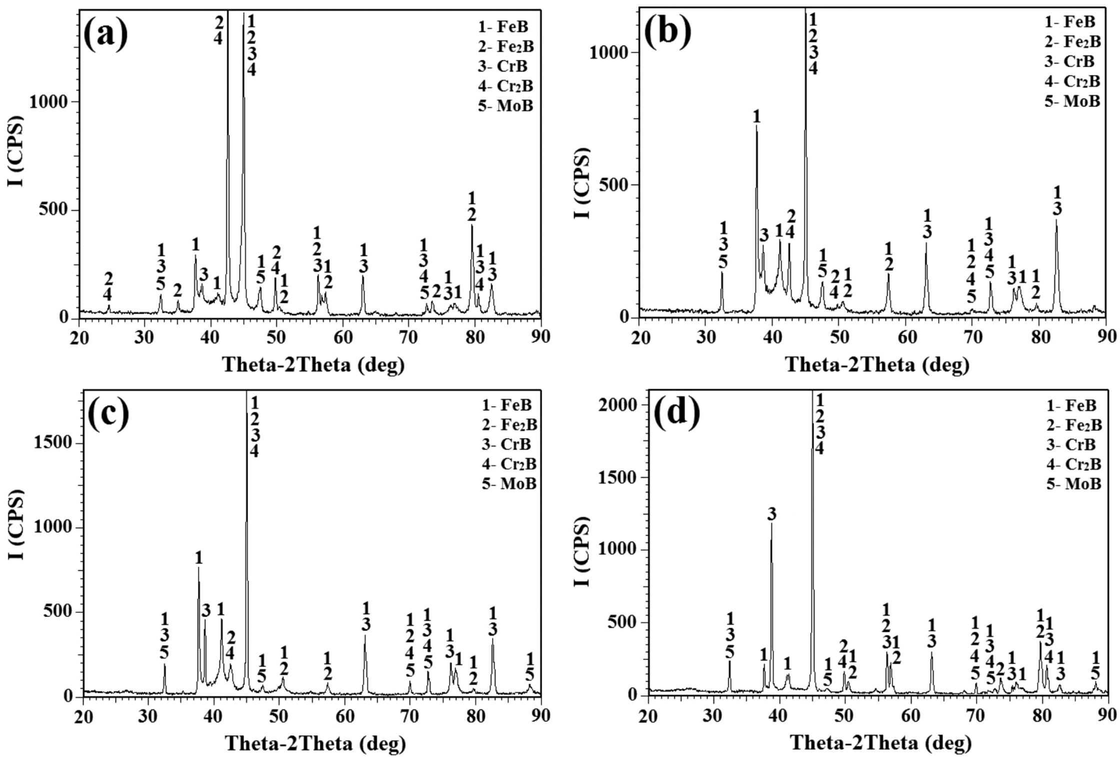

Figure 4: X-ray diffraction patterns of borided AISI H10 steel: a) 1123 K – 2 h, b) 1123 K – 6 h, c) 1223 K – 2 h, d) 1223 K – 6 h
Slika 4: Rentgenska difrakcija boriranega jekla AISI H10: a) 1123 K – 2 h, b) 1123 K – 6 h, c) 1223 K – 2 h, d) 1223 K – 6 h

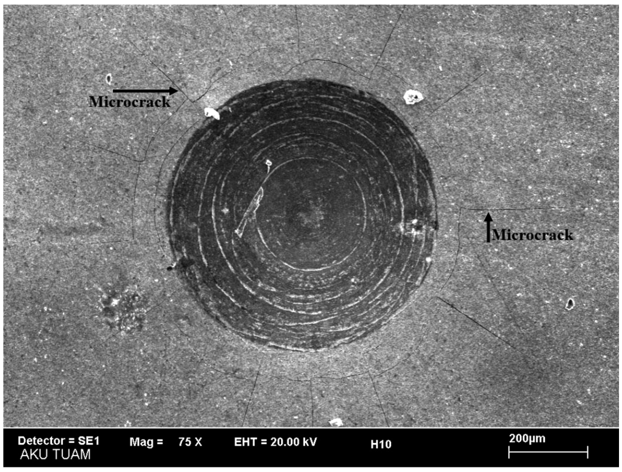

Figure 6: SEM micrograph of VDI adhesion test on AISI H10 steel
Slika 6: SEM-posnetek VDI preizkusa adhezije na jeklu AISI H10

line (**Figure 5**). The microhardness of the boride layers was measured at 10 different locations at the same distance from the surface and the average value was taken as the hardness.

The boride-layer hardness of the sample borided at 1223 K for 6 h was found to be 1964 $HV_{0.05}$, the boride-layer hardness of the sample borided at 1223 K for 2 h was 1816 $HV_{0.05}$, the boride-layer hardness of the sample borided at 1123 K for 6 h was 1765 $HV_{0.05}$, while the boride-layer hardness of the sample borided at 1123 K for 2 h was 1648 $HV_{0.05}$. On the other hand, the Vickers hardness values were 306 $HV_{0.05}$, for the untreated AISI H10 steel. **Figure 5** shows that increasing the boriding temperature and treatment time increases the boride-layer hardness. When the hardness of the boride layer is compared with the matrix, the boride-layer hardness is approximately five times greater than that of the matrix.

3.2 Rockwell-C adhesion

A standard Rockwell-C hardness tester was employed in this study. The damage to the boride layer was compared with the adhesion-strength quality maps HF1–HF6. In general, the adhesion-strength quality HF1–HF4 defines sufficient adhesion, whereas HF5 and HF6 represent insufficient adhesion.[15] SEM micrographs of the indentation craters for the samples borided at 1223 K for 6 h are given in **Figure 6**. There were radial cracks at the perimeter of the indentation craters without flaking and the adhesion of the boride layer on the sample borided at 1223 K for 6 h was sufficient. The adhesion-strength quality of this boride layer is related to HF1.

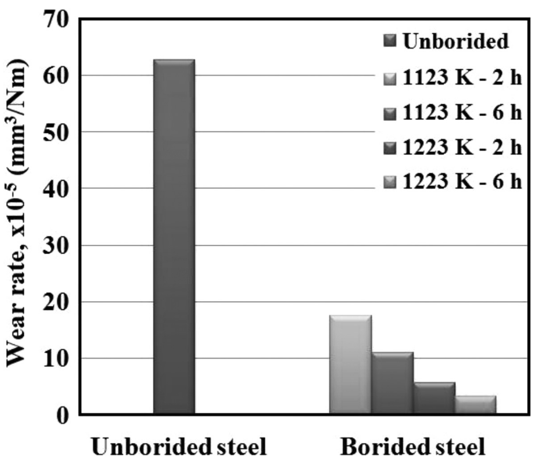

Figure 7: The wear rate of non-borided and borided AISI H10 steel
Slika 7: Hitrost obrabe neboriranega in boriranega jekla AISI H10

3.3 Friction and wear behavior

Table 1 shows the surface-roughness values of the borided and non-borided AISI H10 steel.

The surface roughness of the sample borided at 1123 K for 2 h was found to be 0.34 μm, the boride-layer hardness of the sample borided at 1223 K for 6 h was 0.39 μm, the boride-layer hardness of the sample borided at 1223 K for 2 h was 0.45 μm, while the boride-layer hardness of the sample borided at 1223 K for 6 h was 0.52 μm. On the other hand, the surface-roughness value was 0.09 μm for the untreated AISI H10 steel. **Table 1** shows that increasing the boriding temperature and treatment time increases the surface-roughness values. For the AISI H10 steel it was observed that the surface-roughness values increased with the boriding treatment.

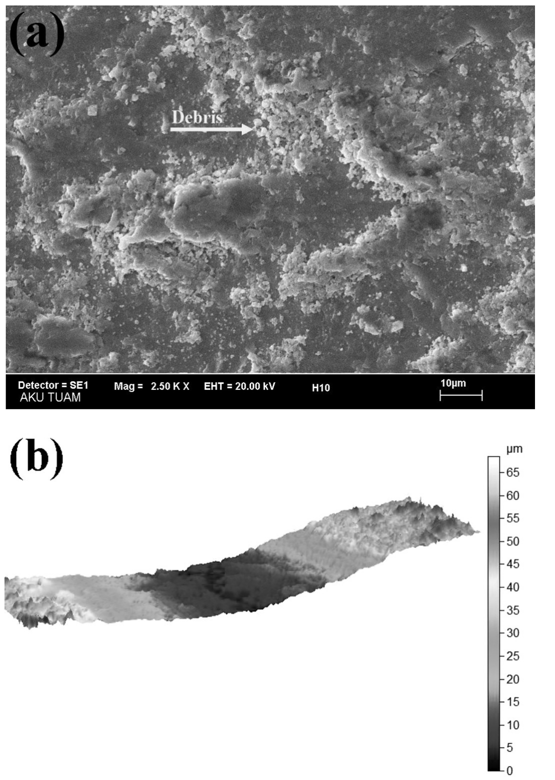

Figure 8: SEM micrograph and cross-sectional surface of the worn-out surfaces of the non-borided AISI H10 steel: a) non-borided, b) cross-sectional surface (CS)
Slika 8: SEM-posnetek in presek obrabljene površine neboriranega jekla AISI H10: a) neborirano, b) presek površine (CS)

Gunes[22] and Sahin[23] reported that the surface-roughness values increased with an increase in the boriding temperature.

Table 1: Surface-roughness values of the non-borided and borided AISI H10 steel

Tabela 1: Vrednosti hrapavosti površine neboriranega in boriranega jekla AISI H10

Unborided	Borided			
	1123 K – 2 h	1123 K – 6 h	1223 K – 2 h	1223 K – 6 h
0.09	0.34	0.39	0.45	0.52

Figure 7 shows the wear rate of the non-borided and borided AISI H10 steel. Reductions in the wear rates of the borided steels were observed according to the non-borided steels. Due to the hardness of the FeB and CrB phases, the steel showed more resistance to wear. The lowest wear rate was obtained in the AISI H10 steel borided at 1223 K for 6 h, while the highest wear rate was obtained in the non-borided AISI H10 steel. The wear-test results indicated that the wear resistance of the borided steels increased considerably with the boriding treatment and time. It is well known that the hardness of the boride layer plays an important role in the improvement of the wear resistance. As shown in **Figures 5** and **7**, the relationship between the surface microhardness and the wear resistance of the borided samples also confirms that the wear resistance was improved with the increasing hardness. This is in agreement with reports of previous studies.[9,23–25] When the wear rate of the borided steel is compared with the non-borided steel, the wear rate of the borided steels is approximately five times lower than that of the non-borided steels.

Table 2: The friction coefficients of the non-borided and borided AISI H10 steel

Tabela 2: Koeficienti trenja neboriranega in boriranega jekla AISI H10

Unborided	Borided			
	1123 K – 2 h	1123 K – 6 h	1223 K – 2 h	1223 K – 6 h
0.64	0.38	0.44	0.48	0.53

The SEM micrographs of the worn surfaces of the non-borided and borided AISI H10 steel are illustrated in **Figures 8** and **9**. **Figure 8a** shows the SEM micrographs of the wear surfaces of the non-borided AISI H10 steel. In **Figure 8a**, the worn surface of the non-borided steel was rougher and coarser wear-debris particles were present. The wear region of the borided steel, debris, delamination wear, surface grooves and cracks on the surface can be observed (**Figure 9**). There were micro-cracks, abrasive particles and small holes on the worn surface of the boride coatings. In the wear region of the borided AISI H10 steel, there were cavities probably formed as a result of layer fatigue (**Figure 9**) and cracks concluded in delaminating wear. **Figure 9** show the wear surfaces and the cross-sectional surface (CS) of a wear mark obtained from the wear region by analyzing multiple profilometry surface line scans using a Nanovea ST-400 non-contact optical profiler. It was observed that the depth and width of the wear trace on the surfaces of the samples decreased with an increase in the boriding temperature and time (**Figure 9**). **Figure 9** shows the EDS analysis obtained from **Figure 9g**. Fe-based oxide layers formed as a result of the wear test. The spallation

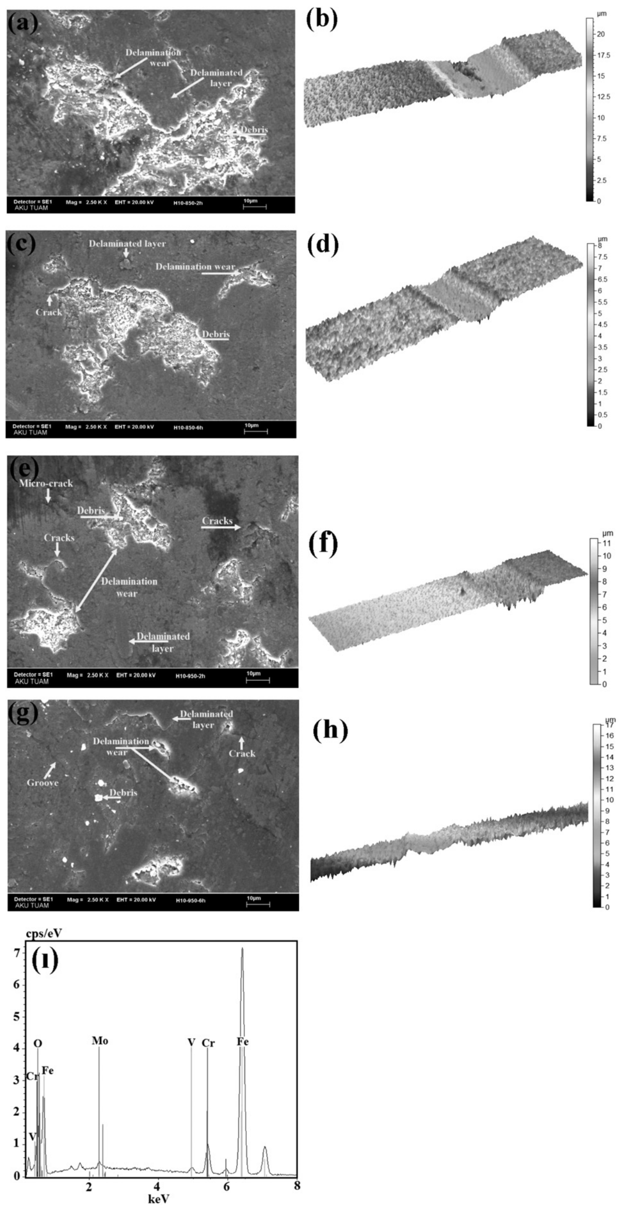

Figure 9: SEM micrographs and cross-sectional surface of the worn-out surfaces of the borided AISI H10 steel: a) 1123 K – 2 h, b) 1123 K – 2 h CS, c) 1123 K – 6 h, d) 1123 K – 6 h CS, e) 1223 K – 2 h, f) 1223 K – 2 h CS, g) 1223 K – 6 h, h) 1223 K – 6 h CS, i) EDS analysis

Slika 9: SEM-posnetki in preseki obrabljene površine boriranega jekla AISI H10: a) 1123 K – 2 h, b) 1123 K – 2 h CS, c) 1123 K – 6 h, d) 1123 K – 6 h CS, e) 1223 K – 2 h, f) 1223 K – 2 h CS, g) 1223 K – 6 h, h) 1223 K – 6 h CS, i) EDS-analiza of the oxide layers in the sliding direction and their orientation extending along the wear track were identified. When the SEM image of the worn surfaces of the non-borided sample is examined, it can be seen that the wear marks in **Figure 8a** are larger and deeper.

4 CONCLUSIONS

In this study, wear behavior and some of the mechanical properties of the boride layer on the surface of borided AISI H10 steel were investigated. Some of the conclusions can be drawn as follows:

- The boride-layer thickness on the surface of the AISI H10 steel was obtained, depending on the boriding time and temperature, 12.86 μm – 63.72 μm;
- The multiphase boride coatings that were thermochemically grown on the AISI H10 steel were composed of the FeB, Fe_2B, CrB, Cr_2B and MoB phases;
- The surface hardness of the borided steel was in the range 1648 $HV_{0.05}$ – 1964 $HV_{0.05}$, while for the untreated the steel substrate it was 306 $HV_{0.05}$;
- The lowest wear rate was obtained in the steel borided at 1223 K for 6 h, while the highest wear rate was obtained for the non-borided steel;
- The wear rate of the borided steel was found to be approximately five times lower the wear rate of the non-borided steel;
- As a result of boriding, the low surface hardness of the AISI H10 steel was improved.

5 REFERENCES

[1] M. Hudakova, M. Kusy, V. Sedlicka, P. Grgač, Analysis of the boronized layer on K190PM tool steel, Mater. Tehnol., 41 (**2007**) 2, 81–84

[2] A. K. Sinha, Boriding (Boronizing) of steels, ASM Handbook, vol. 4, ASM International, 4 (**1991**), 437–447

[3] M. Keddam, Simulation of the growth kinetics of FeB and Fe_2B phases on the AISI M2 borided steel: Effect of the paste thickness, International Journal of Materials Research, 100 (**2009**) 6, 901–905, doi:10.3139/146.110915

[4] S. Ulker, I. Gunes, S. Taktak, Investigation of tribological behaviour of plasma paste boronized of AISI 8620, 52100 and 440C steels, Indian Journal of Engineering and Materials Sciences, 18 (**2011**) 5, 370–376

[5] C. Bindal, A. H. Ucisik, Characterization of borides formed on impurity-controlled chromium-based low alloy steels, Surface and Coatings Technology, 122 (**1999**) 2–3, 208–213, doi:10.1016/S0257-8972(99)00294-7

[6] M. Keddam, R. Chegroune, A model for studying the kinetics of the formation of Fe_2B boride layers at the surface of a gray cast iron, Applied Surface Science, 256 (**2010**) 16, 5025, doi:10.1016/j.apsusc.2010.03.048

[7] I. Gunes, Kinetics of borided gear steels, Sadhana, 38 (**2013**) 3, 527–541, doi:10.1007/s12046-013-0138-0

[8] Z. N. Abdellah, M. Keddam, A. Elias, Evaluation of the effective diffusion coefficient of boron in the Fe2B phase in the presence of chemical stresses, Inter. Journal of Materials Research, 104 (**2013**) 3, 260–265, doi:10.3139/146.110862

[9] I. Gunes, Wear Behaviour of Plasma Paste Boronized of AISI 8620 Steel with Borax and B_2O_3 Paste Mixtures, Journal of Materials Science and Technology, 29 (**2013**) 7, 662–668, doi:10.1016/j.jmst.2013.04.005

[10] E. Garcia-Bustos, M. A. Figueroa-Guadarrama, G. A. Rodríguez-Castro, O. A. Gómez-Vargas, E. A. Gallardo-Hernández, I. Campos-Silva, The wear resistance of boride layers measured by the four-ball test, Surface and Coatings Technology, 215 (**2013**), 241–246, doi:10.1016/j.surfcoat.2012.08.090

[11] T. Leśniewski, S. Krawiec, The effect of ball hardness on four-ball wear test results, Wear, 264 (**2008**) 7–8, 662–670, doi:10.1016/j.wear.2007.06.001

[12] I. Gunes, A. Dalar, Effect of sliding speed on friction and wear behaviour of borided gear steels, Journal of the Balkan Tribological Association, 19 (**2013**) 3, 325–339

[13] T. S. Eyre, Effect of boronising on friction and wear of ferrous metals, Wear, 34 (**1975**) 3, 383–397, doi:10.1016/0043-1648(75)90105-2

[14] S. Sen, U. Sen, C. Bindal, Tribological properties of oxidised boride coatings grown on AISI 4140 steel, Materials Letters, 60 (**2006**) 29–30, 3481–3486, doi:10.1016/j.matlet.2006.03.036

[15] I. Gunes, Tribological behavior and characterization of borided cold-work tool steel, Mater. Tehnol., 48 (**2014**) 5, 765–769

[16] E. Atik, U. Yunker, C. Meriç, The effects of conventional heat treatment and boronizing on abrasive wear and corrosion of SAE 1010, SAE 1040, D2 and 304 steels, Tribology International, 36 (**2003**) 3, 155–161, doi:10.1016/S0301-679X(02)00069-5

[17] Verein Deutscher Ingenieure Normen, VDI 3198, VDI-Verlag, Düsseldorf 1991

[18] N. Vidakis, A. Antoniadis, N. Bilalis, The VDI 3198 indentation test evaluation of a reliable qualitative control for layered compounds, Journal of Mater. Science and Technology, 143–144 (**2003**), 481–485, doi:10.1016/S0924-0136(03)00300-5

[19] S. Taktak, Some mechanical properties of borided AISI H13 and 304 steels, Materials and Design, 28 (**2007**) 6, 1836–1843, doi:10.1016/j.matdes.2006.04.017

[20] I. Gunes, Y. Kayali, Investigation of mechanical properties of borided Nickel 201 alloy, Materials and Design, 53 (**2014**), 577–580, doi:10.1016/j.matdes.2013.07.001

[21] K. L. Johnson, Contact mechanics, Cambridge University Press, Cambridge 1985

[22] I. Gunes, Investigation of Tribological Properties and Characterization of Borided AISI 420 and AISI 5120 Steels, Transactions of the Indian Institute of Metals, 67 (**2014**) 3, 359–365, doi:10.1007/s12666-013-0356-5

[23] S. Şahin, Effects of boronizing process on the surface roughness and dimensions of AISI 1020, AISI 1040 and AISI 2714, Journal of Materials Processing Technology, 209 (**2009**) 4, 1736–1741, doi:10.1016/ j.jmatprotec.2008.04.040

[24] C. Li, B. Shen, G. Li, C. Yang, Effect of boronizing temperature and time on microstructure and abrasion wear resistance of Cr12Mn2V2 high chromium cast iron, Surface and Coatings Technology, 202 (**2008**) 24, 5882–5886, doi:10.1016/j.surfcoat.2008.06.170

[25] D. Mu, B. Shen, X. Zhao, Effects of boronizing on mechanical and dry-sliding wear properties of CoCrMo alloy, Materials and Design, 31 (**2010**) 8, 3933–3936, doi:10.1016/j.matdes.2010.03.024